Journal of the Indian Institute of Science
A Multidisciplinary Reviews Journal
ISSN: 0970-4140 Coden-JIISAD

REVIEWS

Civil Structural Health Monitoring Using FBG Sensors: Trends and Challenges

Umesh Tiwari

Abstract | Structural Health Monitoring (SHM) is a promising and challenging field of research of the 21st century. Civil structures are the most precious economic assets of any country, proper monitoring of these is necessary to prevent any hazardous situation and ensuring safety. Fiber Bragg Grating (FBG) sensors have emerged as a reliable, in situ, non-destructive device for monitoring, diagnostics and control in civil structures. FBG sensors offer several key advantages over other technologies in the structural sensing field. In this article, recent research and development activities in SHM using FBG sensors have been presented. Some of the strain-temperature discrimination techniques recently proposed by us have also been discussed. Distributed strain sensing in a concrete bridge (field trial) using FBG sensors has been presented.

1 Introduction

Civil structures such as buildings, bridges, dams, tunnels, ports, etc. are the most valuable assets of a modern society that need long-term functionality under complex conditions, thus their constant monitoring is pivotal in preventing catastrophe and ensuring safety. Bridges are the lifelines of a nation's infrastructure, and massive investments are being made in the Highway Sector year after year. During the last 50 years, a number of Reinforced Cement Concrete (RCC) and Pre-stressed Cement Concrete (PCC) bridges have been built across the country, and it is estimated that about 25% of them are in some state of distress. Health monitoring of bridges involves strict periodic maintenance procedures, regular visual inspections, and use of conventional sensors, i.e. Electric Strain Gauges (ESGs). Maintenance is expensive (especially when not required) while visual inspections mostly miss out critical problems. ESGs have a number of limitations: (i) they are prone to getting detached from the surface, (ii) there are difficulties with embedding into composites and metallic materials, (iii) many input and output wires are required for quasi-distributed sensing that may compromise the strength of the structure, and are thus susceptible to electromagnetic interference (EMI), (iv) are not suitable for multiplexing and long distance applications, and (v) they have limited life span. Development of fiber optics has led to a significant growth in the field of sensors as they offer several advantages. Fiber Optic Sensors (FOSs) have certain advantages such as their small size, light weight, immunity to EMI, ability to work under harsh environment, suitability for embedding, multiplexing and remote sensing, which make them perfect alternative to ESGs. If protected from breakage they can operate without degradation for decades. Amongst various fiber-sensing technologies, Fiber Bragg Grating (FBG) technology, though comparatively new, constitutes 75% of the fiber optical sensors used in structural health monitoring.[1–3] FBGs are generic sensors that work through creation of strain. Multiple FBGs can be surface mounted and/or embedded for quasi distributed sensing in structures for measuring strain, temperature,[4] cracks[5] and vibrations.[6] They can specify when and what corrective action is needed to repair the structure, thereby avoid large expenditure on unnecessary repair, and timely warning can save damages. Normally, conventional type of embedded sensors provide

CSIR-Central Scientific Instruments Organisation, Sector-30, Chandigarh 160030, India.
uktiwari_2003@yahoo.co.in

static response, thus real time response is obtained using surface measurements, whereas FBG sensors give real time response even under embedded conditions, i.e. internal state of the material can be determined. Experiments on FBG sensors for real time health monitoring of various civil structures are underway in advanced countries for atleast last a decade,[7–12] whereas in Indian context this technology is still in nascent stage. Practical implementation of these sensors requires immediate attention and efforts for their indigenous development. FBGs are intrinsic fiber elements inscribed in photosensitive fibers where index of refraction in the fiber core is periodically modulated by illuminating with UV light. If light from a broadband source is transmitted through such a fiber, one particular wavelength is scattered by this periodic refractive index variation and will be missing from the transmission spectrum. When a light wave enters a medium with varying refractive indices, it undergoes minute reflections from every interface. If all the individual reflections are in phase, then the medium will strongly reflect the incident wave. If the reflected waves are not in phase, the net reflection would be weak. Since the phase difference between adjacent reflections is dependent on the wavelength, it implies that the overall reflection from such a medium would be strongly wavelength dependent. When the reflections from all interfaces add constructively, it leads to the *Bragg Condition* given by

$$\lambda_B = 2n_{\text{eff}}\,\Lambda \text{ (Bragg condition)},$$

where Λ is the pitch of the grating, n_{eff} is the effective refractive index of the core, and λ_B is the Bragg wavelength. Therefore, when light from a broadband source is launched in FBG, the spectral component defined by the above equation is missing from the transmitted spectrum. The Bragg wavelength is shifted if the effective refractive index, or the grating periodicity is changed due to some perturbation;[13,14] in fact both these parameters are directly influenced by strain and ambient temperature. Figure 1 shows the schematic of FBG with back-reflection taking place at a specific wavelength (λ_B).

The change in Bragg wavelength with strain and temperature is given by the equation

$$\frac{\Delta\lambda_B}{\lambda_B} = (1 - p_e)\Delta\varepsilon + (\xi + \alpha)\Delta T$$

where p_e is the effective photoelastic coeff, ξ the thermo-optic coeff, α the thermal expansion coeff, and ε is the deformation in micro strains.

FBGs were fabricated by exposing core of a photosensitive fiber (Fibercore) to intense UV light from a KrF excimer laser at 248 nm.[15] To achieve the FBG with more than 90% reflectivity 7–8 scans were applied. FBG parameter within the appropriate design was monitored using optical spectrum analyzer with broadband ASE source. Figure 2 shows the experimental setup for grating fabrication. To protect the FBG from external environment and to provide strength, the stripped fiber section was re-coated with acrylate. Finally, for the stabilization of FBGs over long period of time, thermal annealing at high temperatures (>150 °C) was carried out.

There are several laboratories in the world that carry out SHM using FBG sensors.[15] The greatest challenge in designing a SHM system is knowing what 'changes' to look for and how to identify them. The characteristics of damage in a particular structure play a key role in defining the architecture of the SHM system. The resulting 'changes' or damage signature will dictate the type of sensors that are required, which in turn determines the requirements for the rest of the components in the system.

There are few other challenges in SHM using FBG sensors, like strain-temperature discrimination, proper bonding and mounting on the surface. Packaging of FBG sensor and their interrogation is also a factor for SHM. In this article,

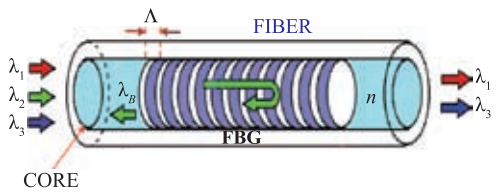

Figure 1: The schematic of an FBG with back reflection taking place at a specific wavelength ($\lambda_2 = \lambda_B$) that satisfies the Bragg condition.

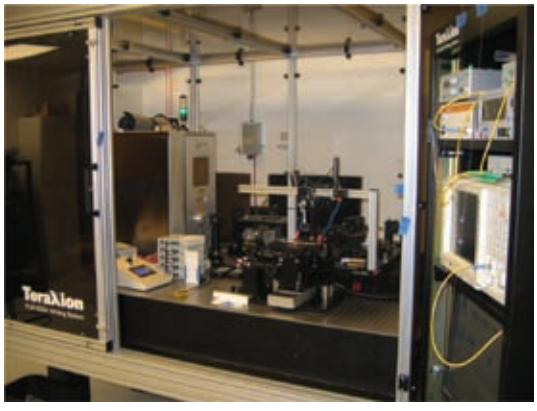

Figure 2: FBG and LPG Writing System.

some of the above issues have been addressed and presented.

2 Packaging and Lab Study of FBG Sensors for SHM

Packaging of FBG sensors is an important aspect owing to its long term usability and handling issues for SHM. FBG sensors have been packaged using appropriately designed and precisely fabricated mild steel fixture, which can respond to the structure perturbations. Figures 3(a) and (b) show the 3D view of FBG packaging fixture and of fabricated FBG fixture made of mild steel, respectively.

We carried out finite element (FEA) analysis of the packaging fixture to investigate the performance on Solid Works Plate form, and the result of one such study is shown in Figure 4. As depicted in the figure, maximum strain occurs at the centre of the fixture when loaded at the centre, the red portion depicts the maximum stress due to bending strain.

We fixed the FBG sensor at the middle of the metallic fixture using glues (CN) and 2-part epoxy (EA-2A) to ensure proper binding and protection of sensor from the ambient. Photograph of the packaged FBG sensor for cementitious mounting/ surface mounting is shown in Figure 5.

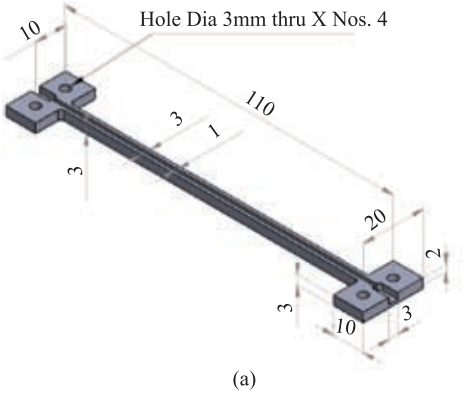

(a)

(b)

Figure 3: (a) 3D design (b) photograph of fabricated FBG packaging fixture.

Conventional strain sensors and packaged FBG sensors in distributed configuration were installed on the surface of the beam at critical locations. A RC beam was subjected to loading as shown in Figure 6, and the responses of FBG sensors were recorded. A typical strain plot by FBG sensors installed in the beams is shown in Figure 7. The trend of the strain variation with the applied load on beam is compatible with strain observed from other sensors.

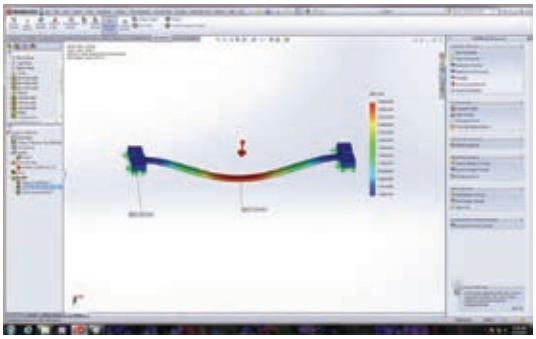

Figure 4: Result of the FE analysis for FBG packing fixture.

Figure 5: Photograph of the packaged FBG sensor for cementitious mounting.

Figure 6: Photograph of RC Beam under test in the laboratory.

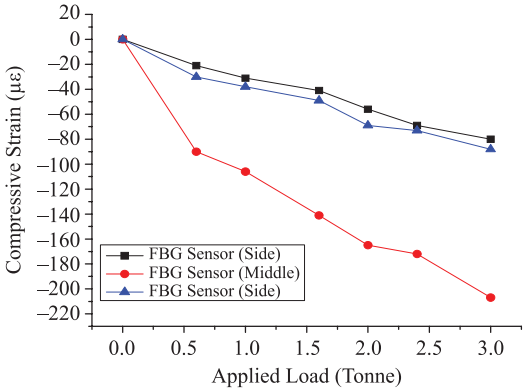

Figure 7: Strain observed by FBG sensors in Beam under compressive load.

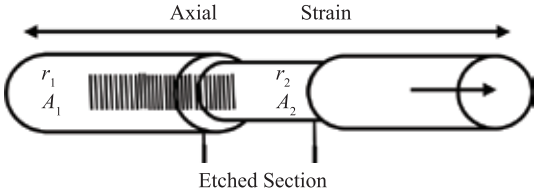

Figure 8: Schematic diagram of the partially etched FBG sensor under longitudinal strain. (r_1, A_1) and (r_2, A_2) denote radius and area of cross sections of non-etched grating (FBG-1) and etched grating (FBG-2) fiber, respectively.

3 Strain-Temperature Discrimination Technique for SHM

Cross sensitivity for strain and temperature measurement in FBG sensors is an important issue. Accurate measurement of strain and temperature requires elimination of cross sensitivity effect. FBG sensor is becoming an integral part of smart structure health monitoring. A considerable number of techniques for temperature and strain discrimination involving FBG sensors has been proposed and demonstrated,[16–25] such as the hybrid FBG/long period fiber grating sensor, superimposed FBGs sensor, using birefringence effect in FBG, etc. There is another type of FBG based sensor that combines FBG with other techniques, such as the FBG cavity sensor,[27] combined fluorescence lifetime decay and FBG technique,[28] extrinsic Fabry–Pérot interferometer combined with chirped in-FBG, using a single-fiber Bragg grating and an erbium-doped fiber amplifier,[29] etc. A simple technique could be the implementation of a combination of two FBGs of different fiber diameters. James et al. (1996) proposed a design by writing grating at the junction of two spliced fibers of slightly different diameters.[30] The spliced FBGs have different thermal and strain sensitivities which make the strain–temperature discrimination model complex.

In the following section, we discuss a single FBG sensor with two sections having significant differences in diameters and a simple analytical model for strain and temperature discrimination with enhanced strain sensitivity. The model is based on one variable of function with diameter of the fiber, and it exploits different strain responses of the gratings due to large mismatch in diameters made by partial etching of the FBG in HF solution. The enhanced strain sensitivity should reduce the error in strain and temperature discrimination. The measured strain and temperature obtained experimentally using our model closely match the applied values. The sensor also has potential to discriminate nano-order strain from temperature depending upon the reduced diameter of the etched part of the fiber.

The design of the proposed FBG sensor is schematically shown in Figure 8. Bragg wavelength of the FBG is chosen as 1550.568 nm. A section, one half of the length of the FBG, is etched in 48% HF solution to reduce its diameter. The diameter of the etched part is monitored by etching time with an etching rate of 3.1 μm/min at room temperature. The area of the cross sections of the non-etched and etched part is denoted by A1 and A2, respectively. It is understood that the strain response of the grating in the etched part will be different from that of the non-etched part due to the difference in diameter in two sections. The working principle of the proposed sensing scheme is based on the relation $\Delta\varepsilon \propto 1/\pi r^2$ between strain and radius of the FBG.

Therefore, the shift in center wavelengths for FBG-1 (Section-A_1) and FBG-2 (Section-A_2) due to both change in longitudinal strains ($\Delta\varepsilon$) and temperatures (ΔT) can be given as[31]

$$\Delta\lambda_{B1} = k_\varepsilon \Delta\varepsilon_1 + k_T \Delta T \quad (1)$$

$$\Delta\lambda_{B2} = k_\varepsilon \Delta\varepsilon_2 + k_T \Delta T \quad (2)$$

where k_ε and k_T are the same for both section of FBG as it is fabricated on the same fiber, and $\Delta\lambda_{B1}$ and $\Delta\lambda_{B2}$ are the shifts of Bragg wavelengths, λ_{B1} and λ_{B2} for FBG-1 and FBG-2, respectively. Since the strain varies with the radius of the fiber as $\Delta\varepsilon \propto 1/\pi r^2$ and r is the radius of the fiber, one can propose a relation between longitudinal strains in two sections of the fiber as[30]

$$\frac{\Delta\varepsilon_1}{\Delta\varepsilon_2} = \frac{A_2}{A_1} \quad (3)$$

where $A_1 (= \pi r_1^2)$ and $A_2 (= \pi r_2^2)$ denote area of cross-sections for non-etched and etched fiber segments

respectively. Subtracting Eq. (1) from Eq. (2) and using Eq. (3) we get:

$$(\Delta\lambda_{B1} - \Delta\lambda_{B2}) = k_{\varepsilon}\left(1 - \frac{A_1}{A_2}\right)\Delta\varepsilon_1 \qquad (4)$$

Knowing the value of k_{ε}, Eq. (4) can be used to determine $\Delta\varepsilon_1$ for given known diameters of the fiber in etched and non-etched sections, provided the shifts $\Delta\lambda_{B1}$ and $\Delta\lambda_{B2}$ are found experimentally. The calculated strain value could be substituted in either Eq. (1) or Eq. (2) to determine the change in temperature. Thus, the sensor can be used to measure strain as well as temperature changes.

As the working principle of the design is based on dependence of strain on area of cross section of the fiber, in order to validate Eq. (3), we first present our experimental results on the measurements of strain response of FBG under a suitable load while reducing diameter of the fiber inscribed with Bragg grating. The diameter of the optical fiber is continuously reduced by etching in HF solution. Figure 9 presents strain and Bragg wavelength shifts as a function of radius of the fiber containing the Bragg grating. The Bragg wavelength shift is continuously monitored during etching of the FBG in 48% HF solution. One end of the grating is connected to FBG interrogator to record the wavelength shifts, while the other end of the fiber carrying a suitable mass hangs inside a plastic tube containing the HF solution. The plastic tube contains certain amount of glycerin at the bottom of the tube; since HF solution is lighter, it floats over the glycerin layer in the tube. The mass hanging from the end of the grating fiber remains inside the glycerin, and, therefore is unaffected by the corrosive HF solution. Finally, etching rate is used to find the respective diameter during the etching period. We used the same mass to theoretically calculate strain as a function of radius. The Young's modulus of the fiber is taken as $Y = 7.18 \times 10^{10}$ N/m^2 for theoretical strain calculation.[32] In Figure 9, we note an excellent match between the two curves showing the variation of wavelength shift and the microstrain with radius of the fiber, showing that the shift in wavelength is proportional to the applied microstrain. In order to validate the relation $\Delta\varepsilon \propto 1/\pi r^2$, we plotted the area of the cross section with change in strain as shown in Figure 10; a linear response is observed. In our experiment, for discrimination of strain and temperature, the FBG is stretched between two holders of a strain measuring station. The applied tension is displayed on a monitor attached to the station. The two ends of the FBG are connected to an Optical Spectrum Analyzer, ANDO-6319 and a light source, respectively. The fiber passes through an aluminum channel which is heated externally. A digital thermometer is attached to the Aluminum channel, close to the FBG, to read temperature of the grating. Wavelength shifts for FBG-1 ($\Delta\lambda_{B1}$) and FBG-2 ($\Delta\lambda_{B2}$) are noted, with changes in temperature and strains.

Figure 11 compares measured strains with the applied strains; Figure 11(a) and 11(b) correspond to $A_1/A_2 \sim 4$ and ~ 17 respectively. The half-filled circles on dotted straight lines are applied strains at different temperatures, while the empty circle point nearest to the half-filled circle point is the respective measured value of the strain. The errors in two cases are within ±13 and ±7$\mu\varepsilon$ over a range of 1700 $\mu\varepsilon$ and 1400 $\mu\varepsilon$ respectively. The temperature sensitivity is 8 pm/°C, as determined from the experiment for the FBG; the measured temperature matches closely with the applied temperature with maximum error of ±1 °C over 60 °C range.

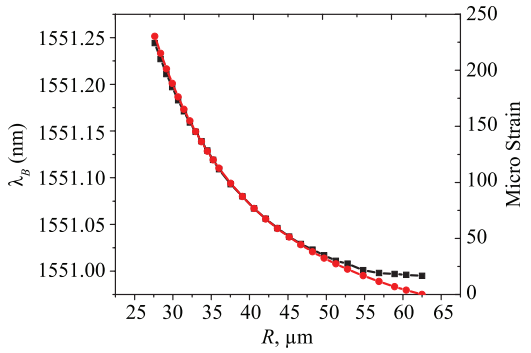

Figure 9: The variation of Bragg wavelength and the microstrain with radius of the fiber, showing that the shift in wavelength is proportional to the applied microstrain.

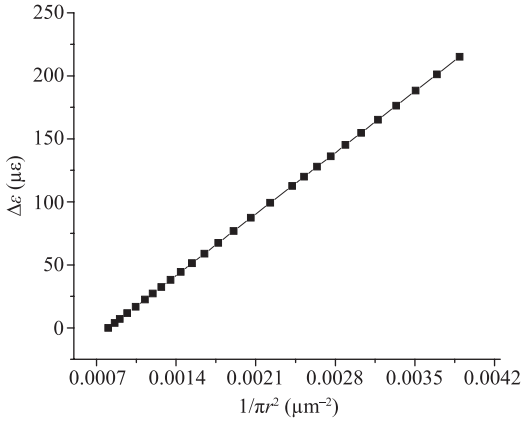

Figure 10: The variation of change in strain with area of the cross section of the fiber, to establish the relation $\Delta\varepsilon \propto 1/\pi r^2$.

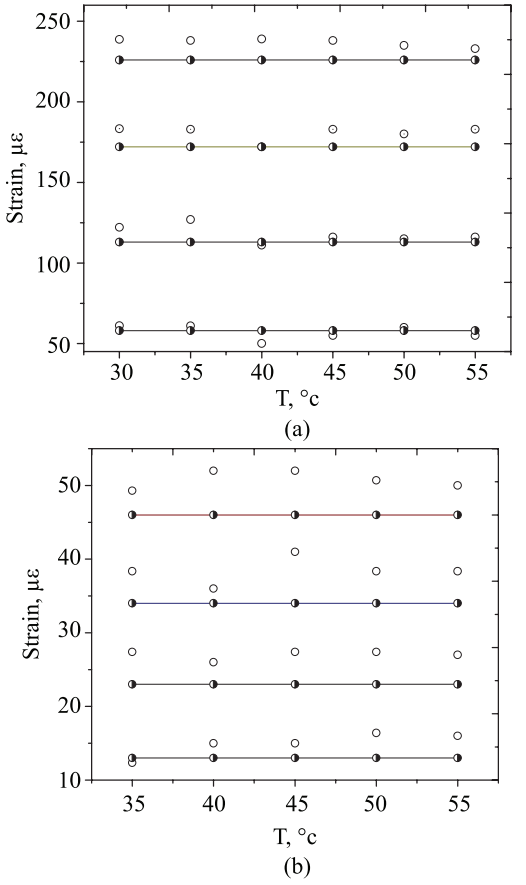

Figure 11: Comparison between applied and measured strains by the proposed model. The half-filled circle points on solid lines are the applied strains at different temperatures. The empty circle point nearest to the half-filled circle point is the respective strain obtained from the model.

4 Field Studies Using FBG Sensors

The girder bridge model was prepared to study the behavior of the bridge under loading conditions on the Solid Works Plateform, and simulated for loading at the center of the bridge using finite element (FEA) analysis. The result of the simulation is shown in Figure 12; the red portion in the figure depicts the maximum stress due to bending strain.

A field study was carried out at the girder bridge near Hapur where conventional and FBG sensors in distributed configuration (arrays/mats pattern) were installed (surface mounted). The schematic layout of the FBG sensors mounted on the surface of the vertical girder at critical locations is shown in Figure 13. The responses of FBG sensors and conventional sensors were recorded under the bridge loading conditions. A photograph of installed sensors on the bridge and the response of FBG sensor at one specific location

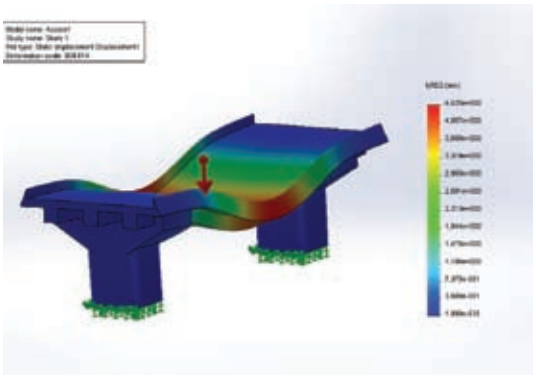

Figure 12: Result of the FE analysis of the girder bridge under loading at the center.

Figure 13: Photograph of the test site of Girder Bridge near Hapur.

Figure 14: Photograph of the close view of the mounted FBG and other conventional sensors.

for different loading under bridge running condition are shown in Figures 14 and 15 respectively. The shift in wavelength of FBG sensor at different locations due to random loading of the bridge whenever heavy vehicles pass through the bridges is shown in Fig. 16.

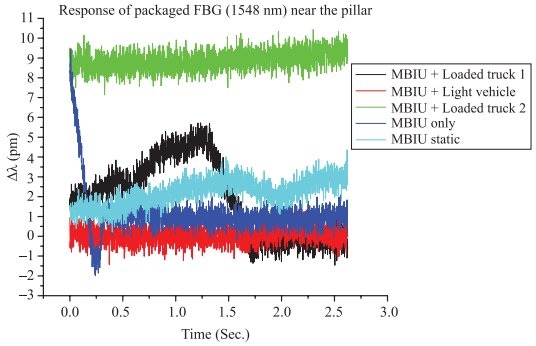

Figure 15: Response of FBG sensor for different loading under bridge running condition.

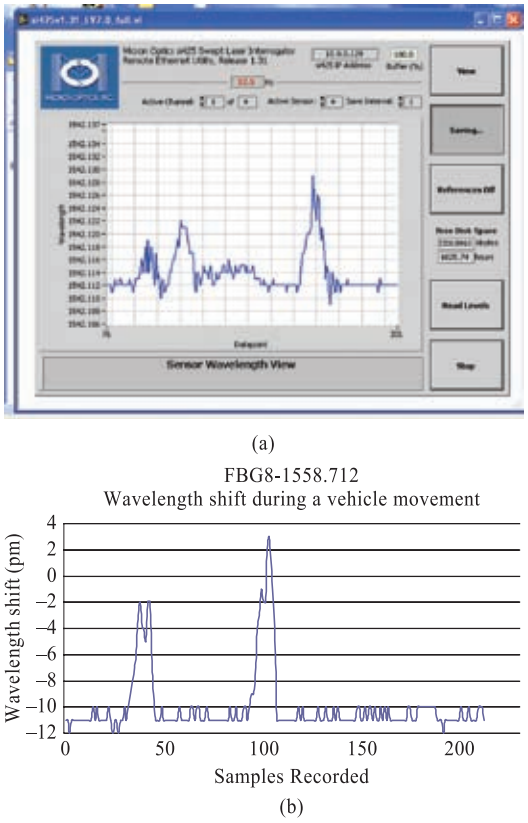

Figure 16: Shift in wavelength in the FBG due to heavy vehicle movement in the specific location.

5 Conclusion

A review of the research and development carried out at CSIR-CSIO for structural health monitoring using FBG sensors is presented. The technology and use behind fabrication, packaging and installation of FBG sensors in the concrete structures have been analyzed. Strain-temperature discrimination technique using a single FBG sensor with two sections of different diameters has been discussed. Field trials with packaged FBG sensor in distributed configuration on concrete bridge have also been demonstrated.

Acknowledgement

Author would like to thank Director CSIR-CSIO Chandigarh, for his support and encouragement. The financial support provided by DST New Delhi is duly acknowledged. Author also thanks to Prof. S. Ashokan, IISc Bangalore, for all his guidance and motivation.

Received 27 June 2014.

References

1. Culshaw, B. and Dakin, J., Optical fiber Sensors, Volume Three, Artech House, 1996.
2. Udd E., Fiber Optic Smart Structures, John Wiley & Sons. Inc., New York, 1995.
3. Kathy K., Optoelectronic Applications: Fiberoptic Sensing—Fiber sensors lay groundwork for structural health monitoring, Laser Focus World, 42(2), 2006.
4. Singh, N., Jain, S.C., Mishra, V., Poddar, G.C., Jindal, V.K., Bajpai, R.P. and Kapur, P., Multiplexing of Fiber Bragg Grating Sensors for Strain and Temperature measurements, Experimental Technique, 2007, 31(3), 54–56.
5. Schulz, W.L., Udd E., Seim J. M. and McGill G. E., Advanced Fiber Grating Strain Sensor Systems for Bridges, Structures and Highways, www.BlueRR.com 1998.
6. Xu Xue-jun and Zhang Xiao-ning, Crack detection of reinforced concrete bridge using video image, Springer 2013.
7. P.F. da Costa Antunes, H.F.T. Lima, N.J. Alberto, H. Rodrigues, P.M.F. Pinto, J. de Lemos Pinto, R.N. Nogueira, H. Varum, A.G. Costa, and P.S. de Brito Andre, Optical Fiber Accelerometer System for Structural Dynamic Monitoring, Sensors Journal, IEEE, 9, 1347–1354, 2009.
8. Rao, Y.J., Recent progress in applications of in-fiber Bragg grating sensors, Optics and Lasers in Engineering, 1999, 31, 297–324.
9. Tenntson, R.C., Mufti, A.A. Rizkalla, S. Tradors G. and Benmokrane, B., Structural Health Monitoring of Innovative Bridges in Canada with Fiber Optic Sensors, Smart Materials and Structures, 2001, 10, 560–573.
10. Majumder, M., Gangopadhyay, T.K., Chakraborty, A.K., Dasgupta, K. and Bhattacharya, D.K., Fiber Bragg Gratings in Structural Health Monitoring-Present Status and Applications, Sensors and Actuators A: Physical, 2008, 147(1), 150–164.
11. Kersey, A.D., Davis, A.M. Patrick, H.J. Michel, Le Blanc, Koo, K.P. and Askins, C.G. et al. Fiber grating sensors, Journal of Lightwave Technology, 1997, 15, 1442–63.
12. Kashyap, R., Fiber Bragg Gratings, (Academic Press, London) 1999.
13. Othonos A. and Kalli K., Fiber Bragg Gratings: Fundamentals and Applications in Telecommunications and Sensing, (Artech House, London), 1999.

14. Singh, N., Jain, S.C., Aggarwal, A.K. and Bajpai, R.P., Fiber Bragg Grating Writing Using Phase Mask Technology, Journal of Scientific Industrial Research, 64, 108–115, 2005.
15. Ou, J.P. and Zhou, Z., Encapsulation techniques for FBG and smart monitoring for bridges with FBG sensors, Proc. of 4th International Workshop on Structural Health Monitoring, Stanford, CA, USA, 2003.
16. Rao, Y.J., In-fiber Bragg grating sensors, Meas. Sci. Technol. 8, 355–362, 1997.
17. Tian, K., Liu, Y. and Wang, Q., Temperature independent fiber Bragg grating strain sensor using bimetal cantilever, Optic. Fiber Technol., 11, 370–377, 2005.
18. Patrick, H.J., Williams, G.M., Kersey, A.D., Pedrazzani, J.R. and Vengsarkar, A.M., Hybrid fiber Bragg grating/long period fiber grating sensor for strain/temperature discrimination, IEEE Photon. Technol. Lett., 8, 1223–1225, 1996.
19. Hsu, Y.S., Wang, L., Liu, W-F. and Chiang, Y.J., Temperature compensation of optical fiber Bragg grating pressure sensor, IEEE Photon. Technol. Lett. 18, 874–756, 2006.
20. Andreas Othonos, Fiber Bragg gratings, Rev. of Scinetific Instrumen. 68, 4309–4341, 1997.
21. Todd, M.D., Jhonson, G.S. and Vohra, S.T. Deployment of fiber Bragg grating-based measurement system in a structural health monitoring application, Smart materials and structures,10, 534–539, 2001.
22. Han, Y.-G., Lee, S.B., Kim, C.-S., Kang, J.U., Paek, U.-C. and Chung, Y., Simultaneous measurement of temperature and strain using dual long-period fiber gratings with controlled temperature and strain sensitivities, Opt. Express, 11, 476–481, 2003.
23. Frazao, O., Romero, R., Araujo, F.M., Ferreira, L.A. and Santos, J.L., Strain-temperature discrimination using a step spectrum profile fiber Bragg grating arrangement, Sensors and Actuators A: Physical, 120, 490–495, 2005.
24. Echevarria, J., Quintela, A., Jauregui, C. and Lopez-Higuera, J.M., Uniform fiber Bragg gratin first- and second-order diffraction wavelength experimental characterization for strain-temperature discrimination, IEEE Photon. Technol. Lett., 13, 696–698, 2001.
25. Guan, B., Tam, H., Ho, S., Chung, W. and Dong, X., Simultaneous strain and temperature measurement using a single fiber Bragg grating, Electronic. Lett, 36, 1018–1019, 2000.
26. Frazão, O., Carvalho, J.P., Ferreira, L.A., Araújo F.M. and Santos, J.L., Discrimination of strain and temperature using Bragg gratings in microstructured and standard optical fibres, Meas. Sci. Technol., 16, 2109–2115, 2005.
27. Du, Wi-C, Tao, X.M., and Tam, H.Y., Fiber Bragg grating cavity sensor for simultaneous measurement of strain and temperature, IEEE Photon. Technol. Lett, 11, 105–107, 1999.
28. Wade, S.A., Forsyth, D.I., Grattan, K.T.V., and Guofu, Q., Fiber optic sensor for dual measurement of temperature and strain using combined fluorescence lifetime decay and fiber Bragg grating technique, Rev. Sci. Instrum. 72, 3186–3190, 2001.
29. Jung, J., Nam, H., Lee, J.H., Park, N., and Lee, B., Simultaneous measurement of strain and temperature by use of a single-fiber Bragg grating and an erbium-doped fiber amplifier, Appl. Optics, 38, 2749–2751, 1999.
30. James, S.W., Dockney, M.L. and Tatam, R.P., Simultaneous independent temperature and strain measurement using in-fiber Bragg grating sensors, Electron. Lett., 32, 1133–1134, 1996.
31. Oh, S.T., Han, W.T., Paek, U.C., and Chung, Y., Discrimination of temperature and strain with a single FBG based on the birefringence effect, Opt. Exp., 12, 724–729, 2004.
32. Pigeon, F., Pelissier, S., Mure-Ravaud, A., Gagnarie, H. and Veillas, C., Optical fiber Young modulus measurement using an optical method, Electron. Lett., 28, 1034–1035, 1992.

Umesh Tiwari received his M.Sc in electronics in 1999 from Bhopal University M.Tech in Optoelectronics in 2004 from SGSITS, Indore and Ph.D. in fiber amplifier and Sensors from IIT Delhi in 2014. He is a recipient of the prestigious CSIR–Young Scientist Award in 2012 in Physical Sciences. His research interests are design and fabrication of FBG/LPG sensors for numerous applications and design and fabrication of EDFA, EDFA/Raman, EDFA/SOA hybrid amplifiers for DWDM application.